

Special Section:

Magnetism in the Geosciences - Advances and Perspectives

Key Points:

- We investigate Miocene glacial dynamics recorded by variations in magnetic properties in the ANDRILL-2A drill core
- Pulses in magnetic mineral concentration reflect changes in sediment transport processes associated with changing glacial conditions
- We refine previous environmental interpretations and delineate a complex early Miocene paleoenvironment in the southern McMurdo Sound

Correspondence to:

 F. Florindo,
 fabio.florindo@ingv.it

Citation:

Jovane, L., Florindo, F., Acton, G., Ohneiser, C., Sagnotti, L., Strada, E., et al. (2019). Miocene glacial dynamics recorded by variations in magnetic properties in the ANDRILL-2A drill core. *Journal of Geophysical Research: Solid Earth*, 124, 2297–2312. <https://doi.org/10.1029/2018JB016865>

Received 11 OCT 2018

Accepted 19 FEB 2019

Accepted article online 26 FEB 2019

Published online 25 MAR 2019

©2019. The Authors.

This is an open access article under the terms of the Creative Commons Attribution-NonCommercial-NoDerivs License, which permits use and distribution in any medium, provided the original work is properly cited, the use is non-commercial and no modifications or adaptations are made.

Miocene Glacial Dynamics Recorded by Variations in Magnetic Properties in the ANDRILL-2A Drill Core

Luigi Jovane^{1,2} , Fabio Florindo^{3,1} , Gary Acton⁴ , Christian Ohneiser⁵ , Leonardo Sagnotti³ , Eleonora Strada³, Kenneth L. Verosub⁶, Gary S. Wilson⁵ , Francesco Iacoviello^{1,7} , Richard H. Levy⁸ , and Sandra Passchier⁹ 

¹Instituto Oceanográfico da Universidade de São Paulo, São Paulo, SP, Brazil, ²Department of Geology, Western Washington University, Bellingham, WA, USA, ³Istituto Nazionale di Geofisica e Vulcanologia, Rome, Italy,

⁴International Ocean Discovery Program, Texas A&M University, College Station, TX, USA, ⁵Department of Geology, University of Otago, Dunedin, New Zealand, ⁶Department of Earth and Planetary Sciences, University of California, Davis, CA, USA, ⁷Department of Chemical Engineering, University College London, London, UK, ⁸Department of Paleontology, GNS Science, Lower Hutt, New Zealand, ⁹Department of Earth and Environmental Sciences, Montclair State University, Montclair, NJ, USA

Abstract During the 2007 ANtarctic geological DRILLing (ANDRILL) campaign in the Ross Sea, Antarctica, the AND-2A core was recovered through a stratigraphic succession spanning 1,138.54 m of Neogene sedimentary rocks that include an expanded early to middle Miocene sequence. The study reported here focuses on the magnetic properties of the interval from 778.63 m below sea floor (mbsf) to 1,138.54 mbsf, which comprises a time interval spanning 1.5 Myr, from ~18.7 to ~20.2 Ma. We recognize three main pulses of increased input of magnetic materials to the drill site between 778.34–903.06, 950.55–995.78, and 1,040–1,103.96 mbsf. Trends in the magnetic mineral concentration dependent parameters mirror changes in the proportion of sediments derived from McMurdo Volcanic Group rocks. We suggest that these pulses in magnetic mineral concentration reflect changes in sediment transport processes associated with changing glacial conditions at the drill site that included (1) subglacial and grounding zone proximal settings, (2) hemipelagic and neritic conditions with abundant sediment-rich icebergs, and (3) grounding zone-distal environment that was covered by land-fast multiyear sea ice or a fringing ice shelf. The magnetic minerals record preserved in the AND-2A core supports other data that indicate a highly dynamic and variable coastal environment during the early Miocene, where glaciers retreated inland under warm climatic conditions and advanced beyond the drill site across the continental shelf when cold climate prevailed.

1. Introduction

Present understanding of Miocene glacial history of Antarctica relies in large part on benthic carbon and oxygen isotope records from deep-sea records, which indicate a highly dynamic glacial environment (e.g., Holbourn et al., 2014, 2015, 2018; Lear et al., 2004; Liebrand et al., 2017; Miller et al., 1991; Shevenell et al., 2008; Zachos et al., 2001). Additional far-field evidence of ice sheet history comes from sequence stratigraphic records on passive continental margins such as Marion Plateau, Australia, and the New Jersey margin, USA, which indicate that sea-level varied up to 100 m, from −60 to +40 m (e.g., John et al., 2011; Kominz et al., 2008, 2016; Miller et al., 1996). Direct evidence of how the ice sheet responded under different climate setting comes from near-field geological records (Antarctic coastal margin), but these records are difficult to obtain because of extensive ice coverage (e.g., Barrett, 1986, 1989; Barrett et al., 2000, 2001; Hambrey & Barrett, 1993; Hambrey & Wise, 1998; Harwood et al., 2009; Naish et al., 2007).

The ANtarctic geological DRILLing (ANDRILL; www.andrill.org) program was established to recover stratigraphic records from the Antarctic continental margin, using drilling technology deployed from ice shelf and sea-ice platforms. During the Southern McMurdo Sound (SMS) Project, a drill core (hereafter referred to AND-2A) was recovered from a location approximately 10 km off the East Antarctic coast in an area that has been influenced by ice sourced from the West Antarctic Ice Sheet and the East Antarctic Ice Sheet (Florindo et al., 2008; Harwood et al., 2009; Figure 1).

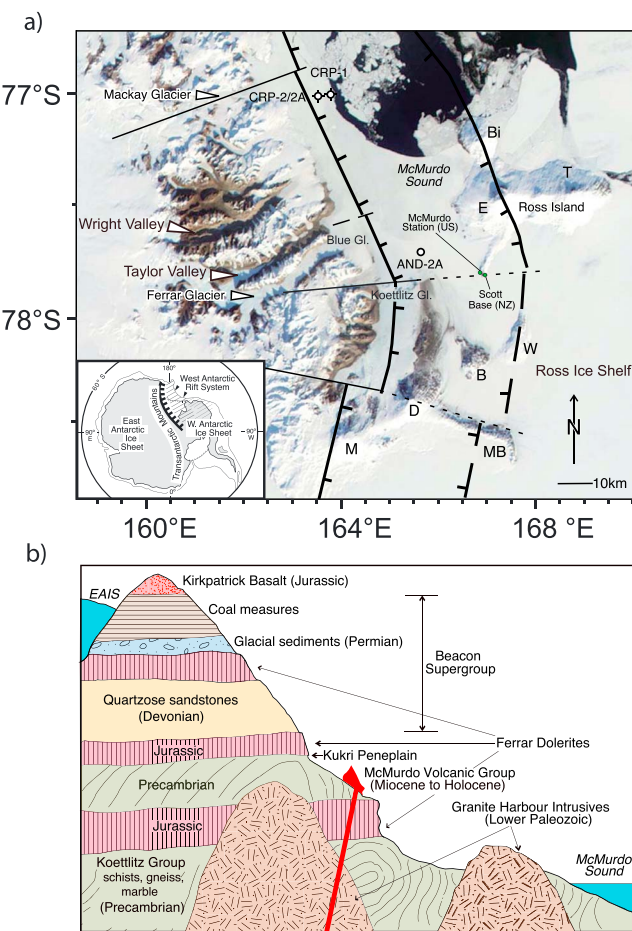


Figure 1. (a) Location of site AND-2A and other drill sites, along with key geographical, geological, and tectonic features in Southern McMurdo Sound. Volcanic centers of the Erebus Volcanic Province include Mt Erebus (E), Mt Terror (T), Mt Bird (Bi), White Island (W), Black island (B), Mt Discovery (D), Mt Morning (M, and Minna Bluff (MB). Boundary faults of the southern extension of Terror Rift are shown (modified from Galeotti et al., 2012). (b) Schematic composite geological cross section showing the morphostratigraphical setting of the investigated area from the East Antarctic Ice Sheet, through the Transantarctic Mountains to McMurdo Sound. After Campbell and Claridge (1987).

(mainly schists, gneisses, and marbles) are intruded by the Granite Harbor Intrusive Complex, which is a suite of lower Paleozoic granitoids (Gunn & Warren, 1962) that mark a subduction phase during the Paleozoic Ross Orogen. A phase of exhumation and protracted erosion of these units during a posttectonic phase led to the development of the Kukri Erosion Surface (Barrett et al., 1972).

A thick sequence of Devonian-Jurassic continental sediments of the Beacon Supergroup sits above the Kukri Erosion Surface (Barrett, 1981; Barrett et al., 1972) and comprises thick units of quartzose sandstone. During the Middle Jurassic, crystalline basement and Beacon Supergroup rocks were intruded by thick dolerite sills and dikes known as Ferrar Dolerites (Harrington, 1958), which are related to the Gondwana breakup (e.g., Bédard et al., 2007; Elliot et al., 1999; Elliot & Fleming, 2000; Zavala et al., 2011).

The McMVG, which surrounds the McMurdo Sound and VLB Basins, consists of several large alkaline stratovolcanoes associated with the West Antarctic rift system (Gunn & Warren, 1962; Kyle, 1990; Figure 1). Eruptions began in the late Oligocene (~26 Ma; Sandroni & Talarico, 2004; Smellie, 2000; Zattin et al., 2012) and became more frequent after ~20 Ma (Di Vincenzo et al., 2010). Mount Morning is the only known source of early to middle Miocene volcanic material recovered from AND-2A core (Di Roberto et al.,

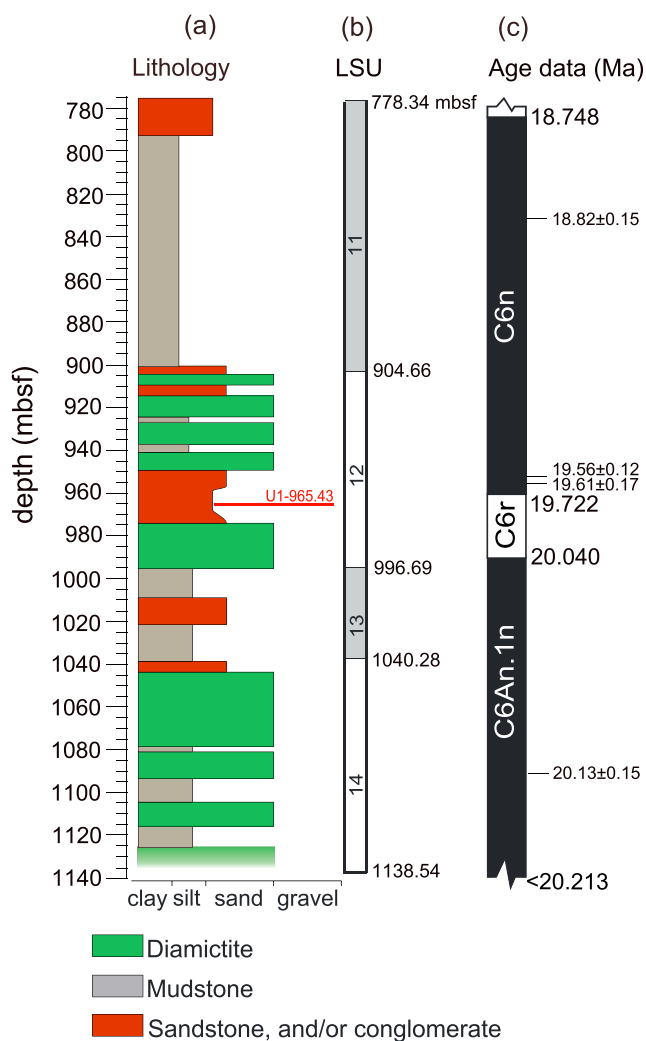
Drilling took place from 10 October through 30 November 2007 and reached a depth of 1,138.54 m below sea floor (mbf) with excellent core recovery (~98%). The stratigraphic section spanned the early Miocene to Pleistocene with an expanded early to middle Miocene section. The record was dated using a combination of biostratigraphy, magnetostratigraphy, $^{40}\text{Ar}/^{39}\text{Ar}$ dates from volcanic clasts, and an Sr-isotope chronology of shell material (Acton, Crampton, Di Vincenzo, et al., 2008; Di Vincenzo et al., 2010; Levy et al., 2016).

The entire stratigraphic section recovered was divided into 14 distinct larger-scale lithostratigraphic units (LSUs) on the basis of major changes in lithology (Field et al., 2018; Fielding et al., 2011; Fielding, Atkins, et al., 2008; Passchier et al., 2011, 2013). We report on mineral magnetic properties from the interval below 778.63 mbf, which encompasses LSUs 11 to 14 spanning approximately 1.5 Myr of the early Miocene, from 18.7 to 20.2 Ma ago (Acton, Crampton, Di Vincenzo, et al., 2008; Levy et al., 2016). These data record environmental variability at the drill site that primarily reflect changes in sediment provenance and augment other proxy data, allowing us to interpret glacial variability through the late early Miocene.

2. Location and Geological Setting

The AND-2A drill core is located approximately 25 km from McMurdo Station and Scott Base and was recovered from a floating sea ice platform in 383-m water depth ($77^{\circ}45.488'\text{S}$, $165^{\circ}16.613'\text{E}$). The drill site is adjacent to the Transantarctic Mountains at the margin of the Victoria Land Basin (VLB; Figure 1), one of the north-south-trending rift basins that constitute the West Antarctic Rift system (e.g., Brancolini et al., 1995; Cooper et al., 1987; Fielding, Atkins, et al., 2008; Henrys et al., 2007; Wilson et al., 2012). Major rifting in the VLB has occurred since the latest Eocene (Fielding et al., 2008), and the basin now contains more than 14 km of Mesozoic and Cenozoic sediments and volcanic detritus. Paleozoic and Mesozoic units in the Transantarctic Mountains and local volcanoes of the late Cenozoic McMurdovian Volcanic Group (McMVG; Kyle, 1990; Wilch et al., 1993) are the main sources of sediments deposited in the VLB (e.g., Cox et al., 2012).

The oldest units in southern Victoria Land are the Precambrian Koettlitz Group metasediments (Grindley & Warren, 1964), which crop out near the Ferrar and Koettlitz glaciers (Figure 1b). The metamorphic rocks



2012; Di Vincenzo et al., 2010; Nyland et al., 2013). Rare outcrops of Miocene to Pliocene glacial, glaciofluvial, and glaciolacustrine sediments occur in the Transantarctic Mountains and their dissecting valleys (e.g., Lewis et al., 2007; Marchant et al., 1996).

3. Core Lithology

The stratigraphic interval below 778.63 mbsf includes LSUs 11 to 14, which span approximately 1.5 Myr, from 18.7 to 20.2 Ma (Acton, Crampton, Di Vincenzo, et al., 2008; Levy et al., 2016; Figure 2). This interval comprises diamictite-dominated units with three subintervals composed of sandstones, mudstones, and siltstones, each with rare gravel occurrences (Fielding et al., 2011; Fielding, Whittaker, et al., 2008). LSU 11 (778.34–904.66 mbsf) is mainly sandy siltstone with dispersed clasts. LSUs 12 (904.66–996.69 mbsf) and 14 (1,040.28–1,138.54 mbsf) are characterized by diamictite with intercalated sandstones, while mudstones, siltstones, and sandstones mainly characterize LSU 13 (996.69–1,040.28 mbsf; Fielding et al., 2011; Fielding, Whittaker, et al., 2008).

A major disconformity, associated to a major ice sheet advanced onto the continental shelf, was identified by Levy et al. (2016) at 965.43 mbsf. Other hiatuses of shorter duration undoubtedly occur in the stratigraphic sequence but are difficult to identify within the resolution of the chronostratigraphic constraints. Sedimentation rates, which average about 18 cm/kyr, were also likely variable given the depositional setting.

4. Sampling, Laboratory Procedures, and Analysis

Paleomagnetic samples were collected from the working half of the split core sections during the sampling party at the Albert P. Crary Science and Engineering Center, McMurdo Station, Antarctica. Core descriptions, provided by the sedimentology logging team, and visual inspection were used in selecting sampling locations, avoiding intervals with pebbles and core deformation and targeted the finer-grained lithologies. A total of 256 samples were collected below 778.63 mbsf at a 1–2-m spacing using plastic boxes in soft sediments and a modified drill press in consolidated sediments (Acton, Crampton, Di Vincenzo, et al., 2008) with sister samples collected every 10 to 20 m.

Low-field low-frequency ($X_{lf} = 0.47$ kHz) and high-frequency ($X_{hf} = 4.7$ kHz) magnetic susceptibility measurements were undertaken at Albert P. Crary Science and Engineering Center, using a Bartington susceptibility meter (model MS2; Acton et al., 2008). After the drilling season, low-field magnetic susceptibility were measured on the same samples using an AGICO KLY-2 Kappabridge magnetic susceptibility meter at the University of California, Davis (USA), Istituto Nazionale di Geofisica e Vulcanologia (Italy), and Otago University (New Zealand) paleomagnetic laboratories. Additional rock magnetic insights come from natural remanent magnetization data from these samples, which were measured at the three paleomagnetic laboratories (University of California, Davis, Istituto Nazionale di Geofisica e Vulcanologia, and Otago University) following stepwise alternating field (AF) demagnetization. In addition, an anhysteretic remanent magnetization (ARM) was imparted by using a 0.05-mT (39.79 A/m) direct current bias field superimposed on a 100-mT peak AF and by translating the samples through the AF and direct current coil system at 10 cm/s. The ARM was then demagnetized at 5, 10, 15, 20, 25, 30, 35, 40, 50, and 60 mT with one magnetic moment measurement made after each three-axis demagnetization step. Magnetic moment measurements were obtained using pass-through cryogenic magnetometers located at the three laboratories (Istituto Nazionale di Geofisica e Vulcanologia, University of California, Davis, and Otago University), using the same translation speed of the trays. Isothermal remanent magnetization acquisition, backfield

Figure 2. Stratigraphic summary of core AND-2A in the interval 778.34–1,138.54 mbsf (modified from Field et al., 2018). (a) Lithology, (b) lithostratigraphic unit (LSU) boundaries, and (c) magnetic polarity record and age data used to establish the AND-2A age model (Levy et al., 2016). The horizontal red line indicates the position of a disconformity, associated to a major ice sheet advance onto the continental shelf (Levy et al., 2016).

susceptibility meter (model MS2; Acton et al., 2008). After the drilling season, low-field magnetic susceptibility were measured on the same samples using an AGICO KLY-2 Kappabridge magnetic susceptibility meter at the University of California, Davis (USA), Istituto Nazionale di Geofisica e Vulcanologia (Italy), and Otago University (New Zealand) paleomagnetic laboratories. Additional rock magnetic insights come from natural remanent magnetization data from these samples, which were measured at the three paleomagnetic laboratories (University of California, Davis, Istituto Nazionale di Geofisica e Vulcanologia, and Otago University) following stepwise alternating field (AF) demagnetization. In addition, an anhysteretic remanent magnetization (ARM) was imparted by using a 0.05-mT (39.79 A/m) direct current bias field superimposed on a 100-mT peak AF and by translating the samples through the AF and direct current coil system at 10 cm/s. The ARM was then demagnetized at 5, 10, 15, 20, 25, 30, 35, 40, 50, and 60 mT with one magnetic moment measurement made after each three-axis demagnetization step. Magnetic moment measurements were obtained using pass-through cryogenic magnetometers located at the three laboratories (Istituto Nazionale di Geofisica e Vulcanologia, University of California, Davis, and Otago University), using the same translation speed of the trays. Isothermal remanent magnetization acquisition, backfield

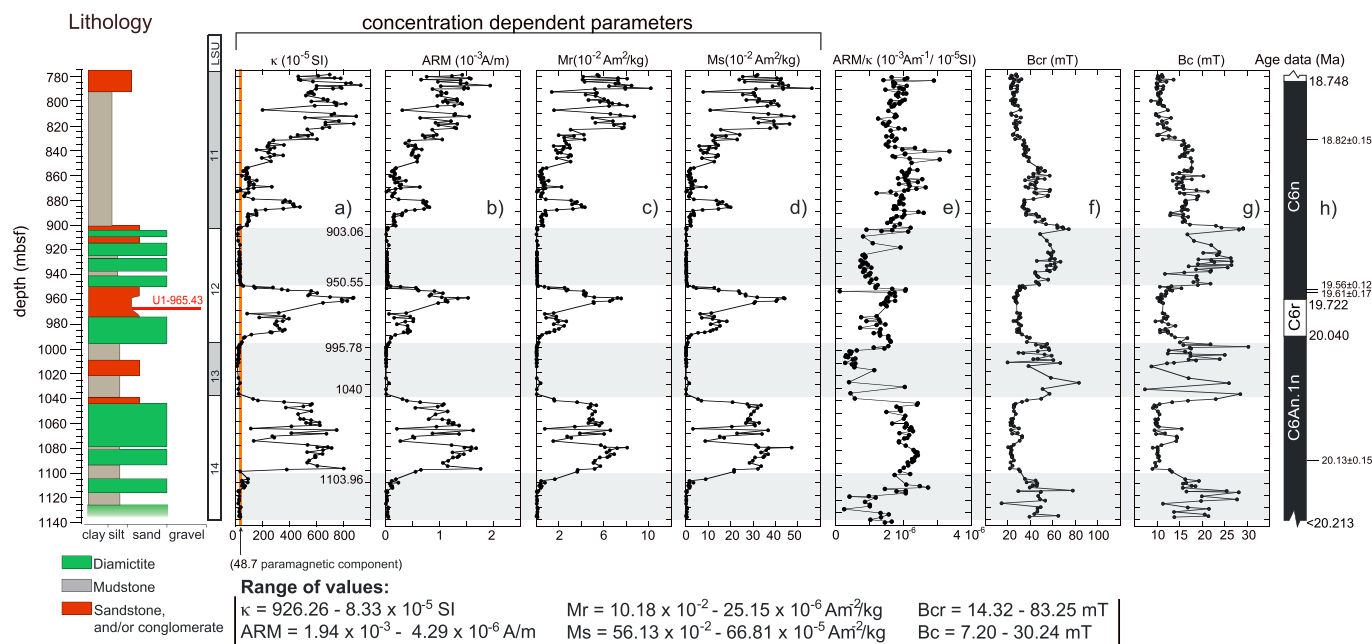


Figure 3. Summary log for the AND-2A core showing mineral magnetic data in the interval 778.34–1,138.54 mbsf. Stratigraphic variation of (a) low-field magnetic susceptibility (κ), (b) anhysteretic remanent magnetization (ARM), (c) saturation remanence (M_r), (d) saturation magnetization (M_s), (e) ARM/ κ ratio, (f) remanent coercivity (B_{cr}), (g) coercive force (B_c), (h) magnetic polarity record and age data for the early Miocene section in AND-2A used to establish the age model (Levy et al., 2016). The horizontal bands in light gray indicate intervals with low concentration of ferrimagnetic minerals.

demagnetization, hysteresis loops, and first-order reversal curve (FORC) measurements (Roberts et al., 2000, 2014) were made on chips from the same samples using a Princeton Measurements Corporation Model 3900 Micromag vibrating sample magnetometer at Western Washington University (USA) and at Centro Estratigráfico de Registros Oceanográfico do Instituto Oceanográfico da Universidade de São Paulo.

On the assumption that magnetite is the prevalent magnetic mineral throughout the section, the ratios of saturation remanence to saturation magnetization (M_r/M_s) and coercivity of remanence to coercive force (B_{cr}/B_c) are useful grain-size indicators of magnetic grains (Day et al., 1977; Dunlop, 2002b, 2002a). For the 22 selected samples, FORC were measured at the Instituto Oceanográfico da Universidade de São Paulo, to investigate in greater detail the magnetic mineralogy. FORC data were corrected and plotted using the FORCinel software (Harrison & Feinberg, 2008).

Temperature dependence of the magnetic susceptibility was measured at Otago University paleomagnetic laboratory on powdered samples with a furnace-equipped KLY-4 (AGICO) Kappabridge, to discriminate ferromagnetic mineralogy. Samples were measured up to a maximum temperature of 700 °C in an argon atmosphere in order to minimize thermochemical alteration in atmospheric oxygen.

5. Results

Magnetic properties alternate between zones with high magnetic intensity and zones with low magnetic intensity. These alternations are used to define six zones of contrasting magnetic properties where an association with the main lithostratigraphic or LSU boundaries in the interval of AND-2A is not straightforward (Figure 3). Susceptibility values range from 926.26×10^{-5} SI to 8.33×10^{-5} SI (Figure 3a), and downcore variations are mirrored by changes in ARM (ranging from 1.94×10^{-3} to 4.29×10^{-6} A/m; Figure 3b), M_r (ranging from 10.18×10^{-2} to 25.15×10^{-6} Am $^{-2}$ /kg), and M_s (ranging from 56.13×10^{-2} to 66.81×10^{-5} Am $^{-2}$ /kg). All of these are concentration-dependent magnetic parameters, which consistently delineate intervals characterized by high and low magnetic mineral concentrations. The concentration of magnetic material is relatively high and variable in the intervals 778.63–903.06 mbsf, 950.55–995.78 mbsf, and 1,040–1,103.96 mbsf, which are referred to as high magnetic-mineral concentration zones (HMMCZs), whereas it is much lower and uniform in the intervening intervals 903.06–950.55, 995.78–

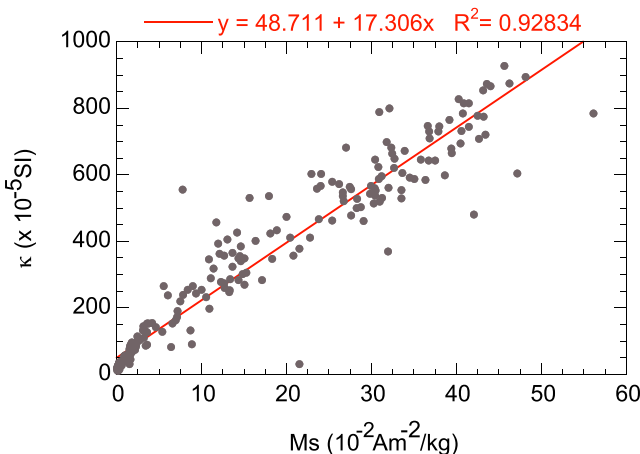


Figure 4. M_s versus κ . The intersection of the regression line with the κ axis provides an estimation of the base level contribution for the paramagnetic susceptibility.

1,040, and 1,103.96–1,138.54 mbsf, which are referred to as low magnetic-mineral concentration zones (LMMCZs). The alternations in magnetic concentration were also noted in the whole-core magnetic susceptibility results made during the ANDRILL-SMS project (see Figure 4 in Dunbar et al., 2008).

By fitting a regression line to a plot of M_s versus susceptibility, we estimate a base-level susceptibility of about 48.7×10^{-5} SI (Figure 4), which we interpret as the paramagnetic component, implying that the three zones of low susceptibility contain little to no ferrimagnetic mineral concentration (Figure 3a).

The ARM/ κ ratio (Figure 3e) is a proxy for magnetic minerals grain size changes in intervals with constant magnetic mineralogy. We observe that the stratigraphic trend of the ARM/ κ parameter mimics those of concentration-dependent parameters, and we infer that this ratio is also controlled by variation in concentration and composition of the mineral magnetic assemblage.

Coercivity of remanence (B_{cr}) and coercivity (B_c) define the same zonation identified by the ferrimagnetic concentration-dependent parameters

(Figures 3f and 3g) but show fluctuations that have an opposite trend and lower amplitude. The hysteresis loops, upon which the coercivities are estimated, are markedly noisier in the LMMCZs because of the low signal to noise ratio (Figure 5).

The coercivity difference between the zones with LMMCZs and the HMMCZs is up to 30 mT. This difference may be a consequence of a significantly reduced content of highly magnetic minerals (i.e., magnetite) in LMMCZs. In fact, in stratigraphic intervals where concentration of magnetite is abundant, subordinate quantities of high coercivity minerals (such as hematite or goethite) are not detectable with most magnetic measurements. Several studies carried out in VLB cores indicate that significant hematite concentrations were observed only in intervals where magnetite concentrations are depleted (e.g., Brachfeld et al., 2013; Roberts et al., 2013; Verosub et al., 2000). We suppose that the input of high-coercivity magnetic minerals from erosion of the Beacon Supergroup and Basement rocks (Figure 1) may have been constant throughout the AND-2A sequence, but their rock magnetic signatures are only visible when the contribution of strongly magnetic grains from the McMVG and Ferrar Group is drastically reduced (Brachfeld et al., 2013). Hysteresis loops have shapes that indicate single domain and pseudo single domain grains with no evidence for the wasp-waisted features typical of mixtures of magnetic minerals with markedly different coercivities (i.e., Bennett & Della Torre, 2005; Kharwanlang & Shukla, 2012; Figure 5d). Isothermal remanent magnetization acquisition and back-field analyses (Figure 5e) are also consistent with the presence of low-coercivity magnetic phases.

Thermomagnetic curves (Figure 6) were produced via progressive heating and show a significant increase in low-field magnetic susceptibility at ~400 °C that we attribute to thermochemical alteration of clay minerals and/or pyrite to magnetite, as indicated by the major drop occurring at 560–580 °C (e.g., Hunt et al., 1995). In any case, the occurrence of magnetite is consistent with prior investigations of similar aged sediments from VLB, which identified detrital magnetite as the mineral that dominates the magnetic properties of these sequences (e.g., Florindo et al., 2005; Roberts et al., 2003, 2013; Sagnotti, Florindo, Verosub, et al., 1998; Sagnotti, Florindo, Verosub, et al., 1998). Authigenic smectites were previously identified by Iacoviello et al. (2012, 2015) in this interval of the AND-2A core. Temperature-dependent susceptibility measurements for a sample at 960.22 mbsf show the presence of other minor peaks at ~230 and ~350 °C, indicating a mixture of other minerals, possibly the iron sulfide mineral greigite and/or titanomagnetite and maghemite, which very commonly occur in volcanic rocks and often are associated with the occurrence of magnetite. Greigite was previously observed in a particularly confined stratigraphic interval of early Miocene age at the base of Cape Roberts Project 1 (CRP-1) drill core (Sagnotti et al., 2005), recovered about 50 km to the north of AND-2A (Figure 1).

The dominance of magnetite is consistent with the AF and thermal demagnetization magnetic behavior observed by Acton, Florindo, et al. (2008) on these sediments. These authors also demonstrated, from

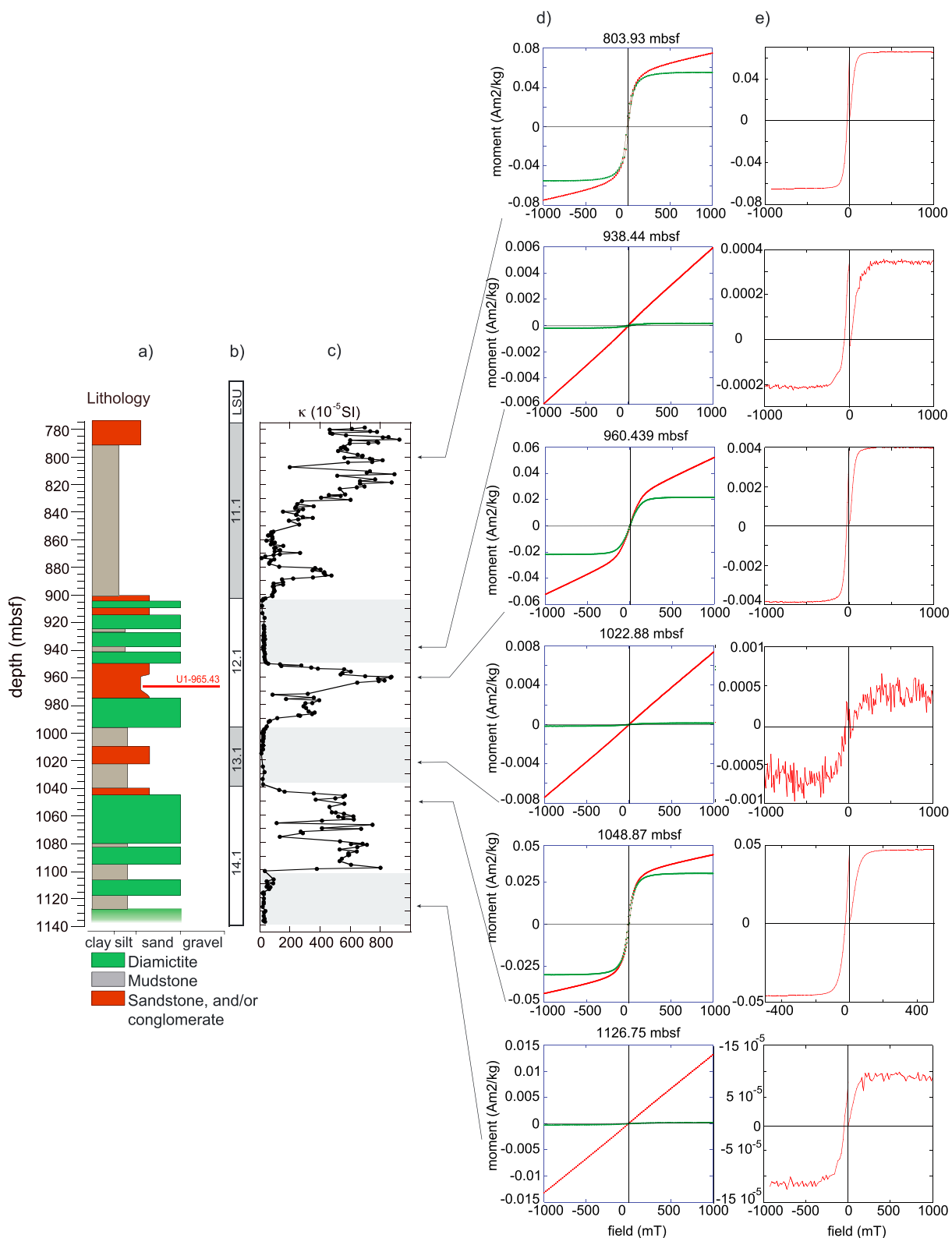


Figure 5. Rock magnetic and stratigraphic summary of core AND-2A in the interval 778.34–1,138.54 mbsf, (a) lithology, (b) lithostratigraphic unit (LSU) boundaries, (c) magnetic susceptibility, (d) hysteresis loops for selected samples (the red and green loops are results before and after subtracting the paramagnetic contribution, by applying an automatic linear slope correction), and (e) isothermal remanent magnetization acquisition and backfield demagnetization analyses.

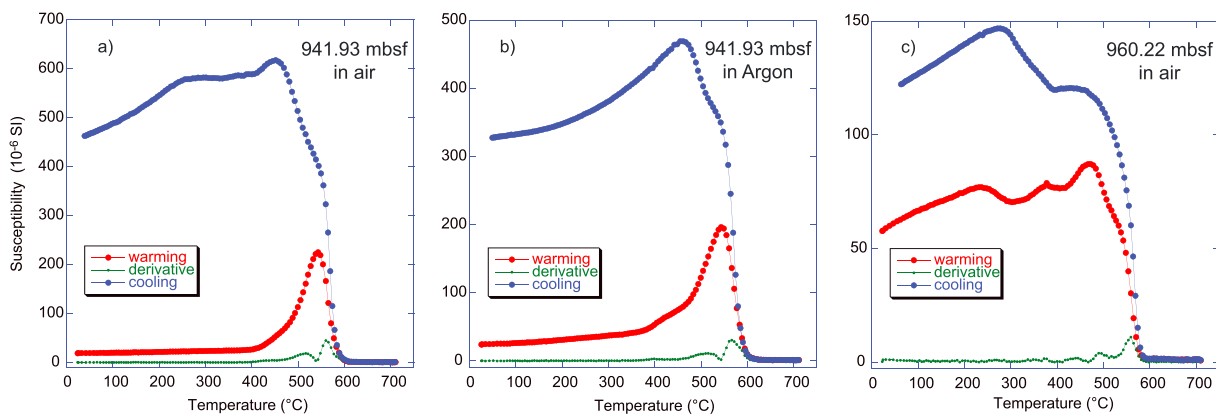


Figure 6. Thermomagnetic curves for samples 941.93 (with argon and open-air atmosphere) and 960.22 mbsf (open-air atmosphere). Low-field magnetic susceptibility is shown for increasing (red) and decreasing (blue) temperatures. First derivative of the warming curve is also represented in green.

the comparison between low-frequency susceptibility and high-frequency susceptibility, that superparamagnetic grains are present at ~3–5%. This finer-grained material was more abundant in zones with lower magnetic mineral concentration.

On the assumption that (titano)magnetite is the dominant magnetic mineral, we investigated the hysteresis data using a Day plot (Day et al., 1977; Dunlop, 2002a) to infer the domain state (Figure 7). The hysteresis ratios (M_{rs}/M_s and B_{cr}/B_c) of nearly all samples from HMMCZs are clustered in a restricted region within the pseudo single domain field, suggesting a relatively constant magnetic grain size for ferrimagnetic (titano)magnetite grains. Samples from LMMCZs show a larger data distribution. We link this scatter both (a) to the lower resolution of the hysteresis loops in samples that are particularly weakly magnetic and (b) to a possible additional contribution from subordinate high-coercivity minerals (whose signal is completely masked by the high content of magnetite in HMMCZs).

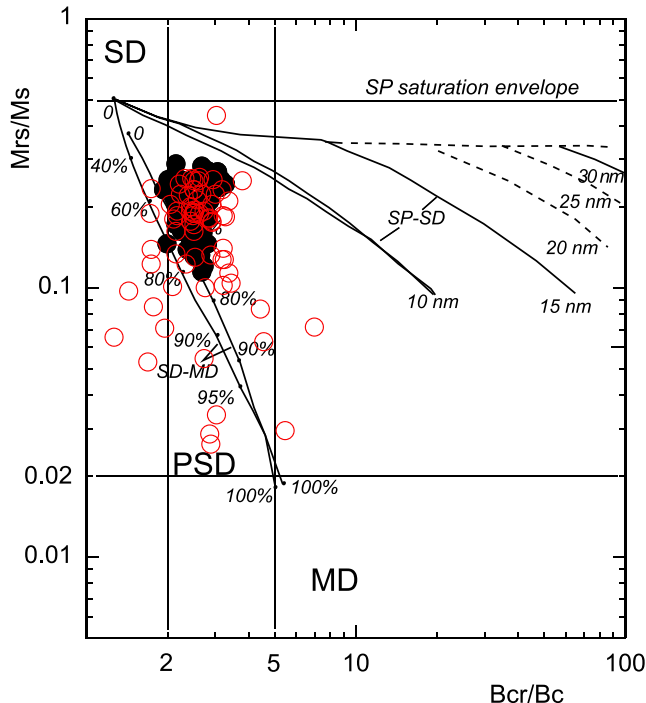


Figure 7. M_{rs}/M_s and B_{cr}/B_c data plotted (solid circles) on theoretical Day plot curves calculated for magnetite. The remanence and the coercivity ratio of these samples can be interpreted as pseudo-single domain magnetite. Samples from the intervals with low concentration of ferrimagnetic minerals are indicated by open circles. Numbers along curves are volume fractions of the soft component (superparamagnetic [SP] or multidomain [MD]) in mixtures with single domain (SD) grains. Curves with SP-SD mixtures have grain sizes indicated for the SP fraction (Dunlop, 2002b, 2002a).

FORC diagrams were produced to characterize magnetostatic interactions and magnetic domain state distributions in the studied samples. They are characterized by maxima for the coercivity spectra of <40 mT and display a small divergence with a triangular shape of outer contours that indicate pseudo single domain grains (e.g., Roberts et al., 2000, 2014; Figure 8). We were not able to obtain meaningful FORC distributions for several of the samples from intervals of low magnetic intensity (e.g., LSU 13 and from the top of LSU 12), even after stacking multiple runs (Heslop & Roberts, 2012).

HMMCZs coincide with increased sand content in the mudstone in LSU 11 (Passchier et al., 2013), sandstone in the lower part of LSU 12 (Passchier et al., 2011), and predominantly sandy diamictite in LSU14. In contrast, LMMCZs coincide with mudstone in LSU 13 and muddy diamictites in the upper part of LSU12 (Passchier et al., 2011). These observations suggest that sand content is an important factor determining the magnetic intensity of the different intervals.

Isothermal remanent magnetization acquisition and thermomagnetic curves in both the LMMCZs and the HMMCZs indicate that magnetite is present as the dominant magnetic mineral but cannot exclude the presence of other magnetic minerals that saturate in magnetic fields of <300 mT or have Curie temperatures of <580 °C. Besides the presence of nearly pure magnetite, it is very likely that magnetite with some

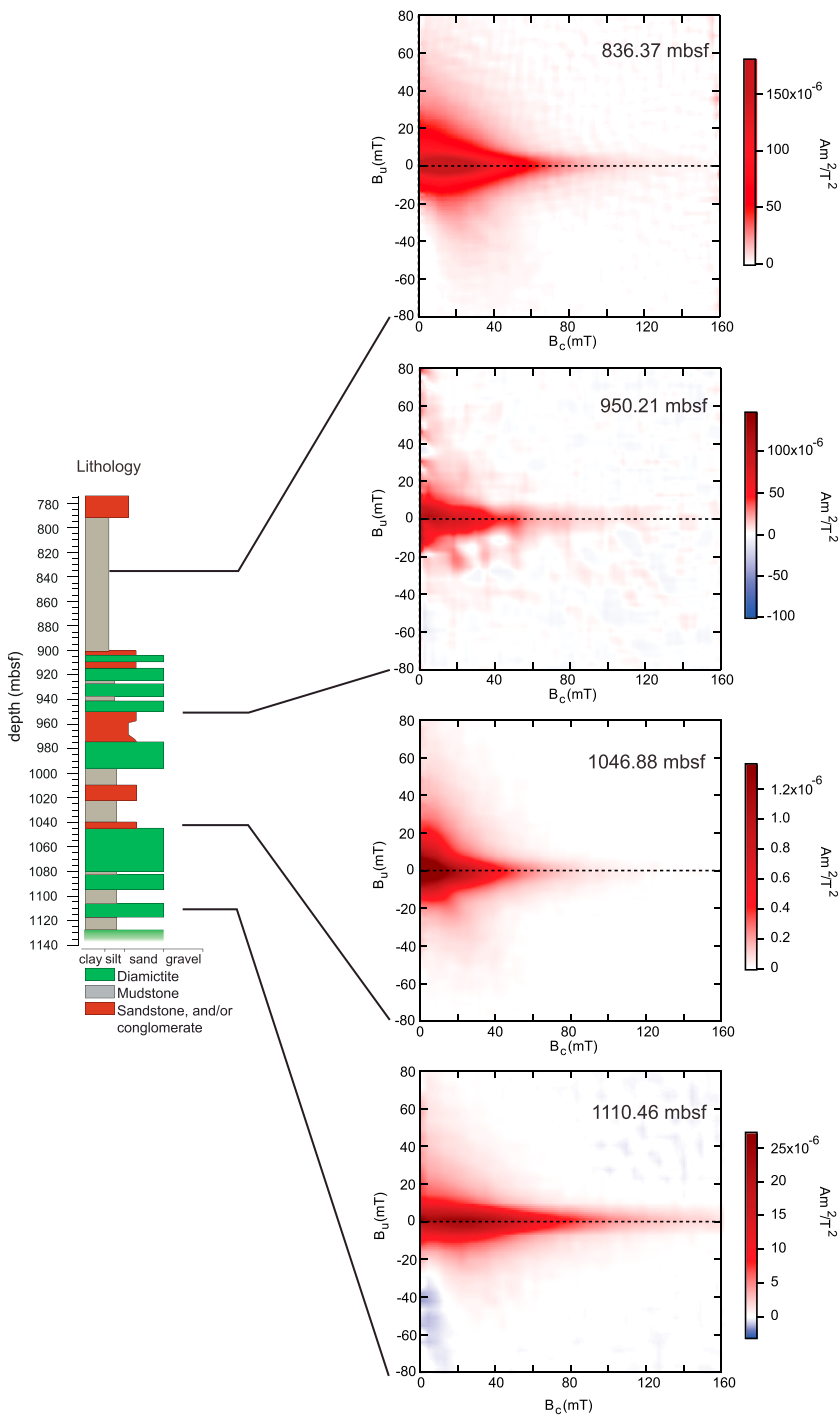


Figure 8. First-order reversal curve (FORC) diagrams for four representative samples. The data were processed using Forcinel software (Harrison & Feinberg, 2008). The small divergence and the triangular shape of outer contours indicate a contribution from the pseudo single domain grains. The smoothing factor is 4 for all FORC diagrams. The vibrating sample magnetometer average time is 0.20 s for sample 950.21 mbsf and 0.10 s for the other three samples displayed.

titanium (titanomagnetite) and/or oxidized magnetite/titanomagnetite (maghemite/titanomagnetite) is present. Both of these minerals are common in volcanic rocks. Volcanic material from the McMVG appears to be the source for the highly magnetic minerals in HMMCZs, with that source being absent or nearly so for the LMMCZs, as we argued before.

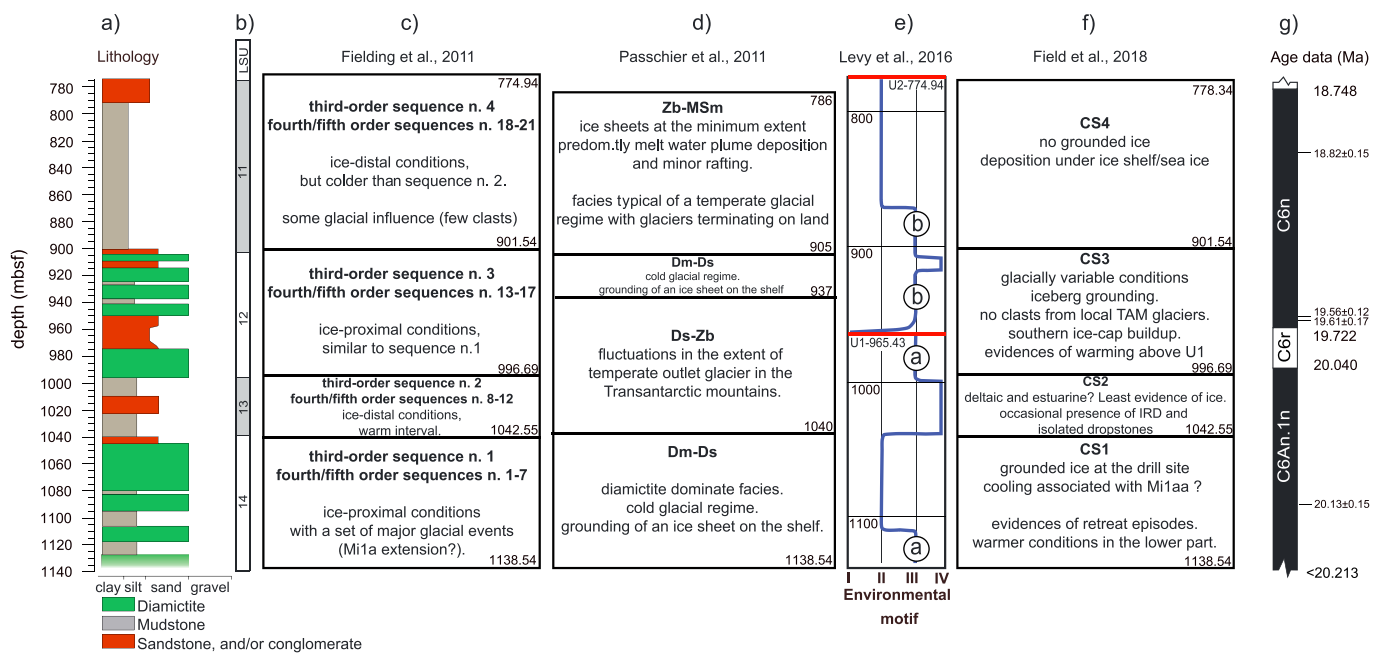


Figure 9. Summary of environmental interpretations of core AND-2A in the interval 778.34–1,138.54 mbsf. (a) Lithology; (b) lithostratigraphic unit boundaries; (c) environmental interpretations from Fielding et al. (2011), (d) from Passchier et al. (2011), (e) from Levy et al. (2016), and (f) from Field et al. (2018); and (g) age data and magnetostratigraphy for the early Miocene section.

6. Previous Environmental Interpretations

Previous studies on the AND-2A core include sequence stratigraphic analysis, detailed sedimentological analyses, sedimentary facies analysis, and integration of multiproxies (Field et al., 2018; Fielding et al., 2011; Levy et al., 2016; Passchier et al., 2011, 2013), and produced slightly different environmental interpretations (Figure 9).

Fielding et al. (2011) recognized a repetitive stratal stacking pattern of lithofacies that was used to divide the entire AND-2A succession into 13 (third-order) glacimarine composite sequences (CSs; Figure 2 in Fielding et al., 2011). The interval studied here includes sequences 1 to 4 (Figure 9c). Sequence 1, between 1,138.54 and 1,042.55 mbsf, records an interval of ice-proximal conditions with a set of major glacial events. CS 2, between 1,042.55 and 996.69 mbsf, is characterized by distal ice conditions (deltaic/estuarine parasequences?) and records a warm interval. Sequence 3, between 996.69 and 901.54 mbsf, has been considered to represent a “cold” environment, similar to that described for sequence 1. CS 4, between 901.54 and 774.94 mbsf, contains the thickest fine-grained interval in the core and has been interpreted to represent another period of ice-distal conditions but colder than CS 2.

Passchier et al. (2011) presented an analysis of facies associations and inferred paleoclimatic conditions for the AND-2A core. Three facies associations were recognized representing three fundamentally different paleoclimatic regimes (Figure 9d). (1) A diamictite dominated facies association (Dm-Ds), between ca. 1,138 and 1,040 mbsf and between ca. 937 and 905 mbsf, indicating a cold glacial regime with the presence of ice shelves and brief periods with ice-free coasts. (2) A stratified diamictite-mudstone association (Ds-Zb), between ca. 1,040 and 937 mbsf, indicating a very dynamic ice sheet and including facies associated with open-marine and iceberg-influenced depositional environments. (3) A mudstone dominates facies association (Zb-MSm) that generally lacks diamictites and is typical of a temperate glacial regime with glaciers terminating on land. This facies association occurs between ca. 905 and 786 mbsf.

Levy et al. (2016), through analysis of an integrated proxy environmental data set, recognized four environmental motifs (EM; Figure 9e) reflecting distinct glacial regimes and two major disconformities through this interval: at 965.43 mbsf (U1; from ~20 to 19.8 Ma) and at 774.94 mbsf (U2; from ~18.7 to 17.8 Ma), which is just above the studied interval. EM I is characterized by maximum ice extent, just above U1 between 965 and

970 mbsf with the Antarctic ice sheet advancing seaward and expanding across the continental shelf. EM II, between 774.94 and 880.06 mbsf and between 1,035.87 and 1,103.96 mbsf, is characterized by colder polar conditions with persistent ice shelves and/or land-fast sea ice along the coast and minimum marine-based grounding line variability. EM III is characterized by subpolar (cold temperate) conditions with a tidewater glacier that calved at the coast, and on the basis of lithofacies variations, it is divided into subtypes a (stratified diamictite) and b (massive and stratified diamictite). Below U1 to about 1,000 mbsf and from 1,103.96 to the bottom interval, an interval of EM IIIa is observed. EM IIIb, from 880.06 to 965.43 mbsf, is characterized by a warmer climate and includes intervals with tundra vegetation along the coast. Minimum ice extent characterizes EM IV, from about 910 to 920 mbsf and from about 1,000 to 1,035.87 mbsf. EM IV records times when a grounded glacier retreated inland and tundra vegetation developed along the coast (e.g., Lewis & Ashworth, 2015).

Recently, Field et al. (2018) presented detailed sedimentological data from AND-2A that showed significant variability in Antarctic ice sheet extent during the early Miocene. From the stratigraphic interval below 778.63 mbsf, four CSs were recognized (CS1–CS4), which are comparable with LSUs 14–11 of Fielding, Whittaker, et al. (2008; Figure 9h).

The oldest phase of diamictite deposition, CS 1 (1,138.54–1,052.55 mbsf; 20.2 to 20.1 Ma), indicates grounded ice at the drill site, and it could be linked to the cooling phase associated to isotope event Mi1aa (Miller et al., 1991; Pekar & DeConto, 2006). This diamictite package includes finer-grained intervals that are interpreted to indicate episodes of distal or retreating ice. Increased carbonate content below ~1,105 mbsf indicates warmer or perhaps less corrosive ocean waters during this time compared with the upper half of the sequence.

This sequence is overlain by sediments that were deposited during the warmest phase of the early Miocene. CS 2 (1,042.55–996.69 mbsf; age range between 20.1 and 20.05 Ma) is a sandstone-, siltstone-, and mudstone-dominated interval with no diamictites. Compared with CS1, this sequence is inferred to indicate substantial warming and more ice-distal conditions. Isolated dropstones and rare ice rafted debris indicate marine-based glaciers, or perhaps ice shelf were present in the area.

CS 3 (996.69–901.54 mbsf; age range between 19.9 and 19.4 Ma), comprises a new pulse of diamictite accumulation, with indicators of occasional ice grounding at the drill site (grounded icebergs?), which is inferred to record ice advance. Increased carbonate content above the unconformity inferred by Levy et al. (2016) suggests relatively warmer conditions than below.

The approximately 100-m-thick mud-rich unit CS 4 (778.34–901.54 mbsf; age range from 19.4 to 18.7 Ma) contains dispersed clasts, which indicates that sea ice, ice shelf, or icebergs were present particularly in the upper part of CS4. Chewings et al. (2011) identified dispersed granules in pebble and/or cobble free units, which they suggested to indicate sediment transport over sea ice by wind during the summer.

7. Discussion

Before recovery of the AND-2A succession, the only other proximal early Miocene successions from the western Ross Sea area were drilled during Cape Roberts Projects 1 and 2 (CRP-1 and CRP-2/2A; e.g., Barrett, 1998; Barrett et al., 2000; Figure 1).

The CRP-1 drill core included an interval of Quaternary sediments between 16 and 43.55 mbsf and an interval of early Miocene sediments between 43.55 mbsf and the bottom of the hole at 147.69 mbsf (e.g., Florindo et al., 2005; Roberts et al., 1998). Magnetic properties of the early Miocene sediments show similar alternation of intervals with high and low concentrations of detrital magnetite that were hypothesized to reflect changes in detrital input linked to fluctuations in the position of the termini of temperate glaciers (Roberts et al., 2013; Sagnotti, Florindo, Wilson, et al., 1998).

The sedimentary succession recovered in the CRP-2/2A drill core comprised a 597-m succession of early Oligocene through early Miocene alternating glacial and interglacial strata overlain by a 27-m succession of mainly glacial Pliocene-Quaternary sediments. The early Miocene succession spanned between approximately 186 and 27 mbsf (Cape Roberts Science Team, 1999; Florindo et al., 2005; Wilson, Bohaty, et al., 2000; Wilson, Florindo, et al., 2000; Wilson et al., 2002). Magnetic properties of the early Miocene interval of CRP-2/2A also show a dominance of detrital magnetite with alternating intervals of high and low values

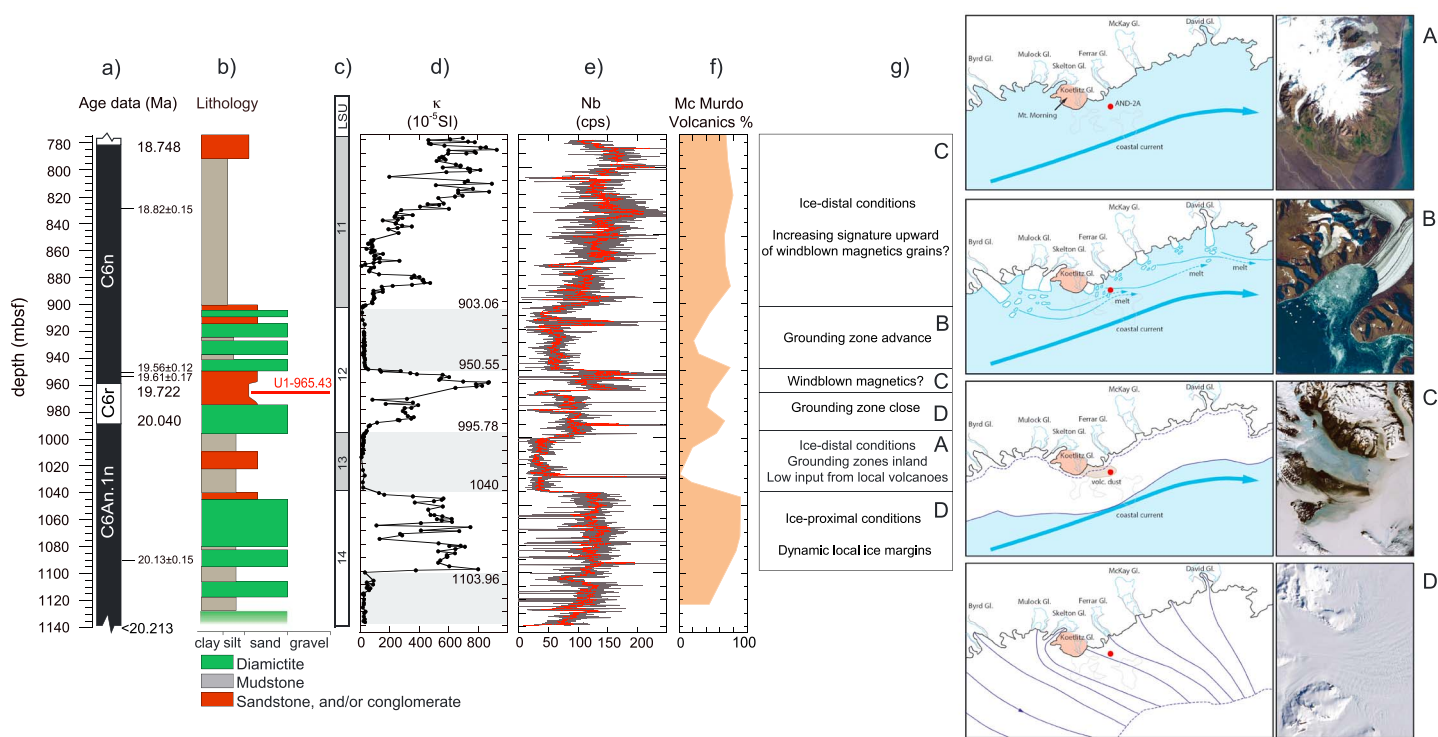


Figure 10. Relationship between rock magnetic data and environmental conditions. (a) Age data and magnetostratigraphy for the early Miocene section, (b) stratigraphic summary of core AND-2A in the interval 778.34–1,138.54 mbsf, (c) lithostratigraphic unit boundaries, (d) magnetic susceptibility, (e) niobium X-ray fluorescence core scanner (XRF-CS) counts, reflecting changes in sand-sized detrital sediment content derived from McMurdo Volcanic Group rocks (Roser & Pyne, 1989; Iacoviello et al., 2015; Levy et al., 2016) with 10 data points moving average, (f) contribution of McMurdo volcanics to the relative abundances of the heavy mineral assemblages in the core (Iacoviello et al., 2015), and (g) reconstructions of glacial configurations inferred for four different coastal environments as characterized by distinct magnetic signatures recorded in the AND-2A drill core.

of concentration-dependent magnetic parameters, associated with high and low concentrations of volcanic glass from the McMVG. This correlation was interpreted to indicate that the magnetic properties provided a record of changes in the supply of fine-grained particles from the McMVG (Roberts et al., 2013; Verosub et al., 2000), which may also have been associated with changing glacial conditions at the drill site. The picture that emerges from the AND-2A core, and from the environmental interpretations described in section 6, is of a highly dynamic Antarctic ice sheet during the early Miocene where during cool periods the grounded ice expanded farther than today and during prolonged warm periods retreated significantly leaving ice-free conditions at the AND-2A site. As shown in other similar studies (e.g., Sagnotti, Florindo, Verosub, et al., 1998; Sagnotti, Florindo, Wilson, et al., 1998; Brachfeld et al., 2013; Roberts et al., 2013), environmental magnetism can provide additional data that help identify and evaluate past environmental and climatic changes (Liu et al., 2012, and references therein).

The environmental magnetic record in AND-2A reveals intervals with high- and low-magnetic mineral (magnetite) concentrations and a relatively constant magnetic grain size with a clear association to lithofacies (Figures 3 and 10). These fluctuations closely mirror variations in Niobium (Nb) content and relative abundances of the heavy mineral assemblages (Iacoviello et al., 2015; Figure 10), both reflecting changes in sand-sized detrital sediment content derived from McMVG rocks (Roser & Pyne, 1989). Ohneiser et al. (2015) characterized the magnetic properties of southern Victoria Land lithologies, which allow us to further link changes in magnetic properties in the AND-2A core with the regional rock groups.

Figure 10 shows that different lithofacies in AND-2A are characterized by distinct ranges in magnetic susceptibility (representing the concentration-dependent magnetic parameters), Niobium content, and percentage of Mc Murdo volcanics that suggest changes in sediment provenance and reflect different glacial environments at the drill site. These distinct units and their associated depositional environments include the following:

- (1) Sandy siltstone and siltstone units with low magnetic susceptibility and Nb content (e.g., from 995.78 to 1,040 mbsf) reflect little input from volcanic sources (Figure 10g, inset A). Glacial grounding zones retreated inland from the coast and exposed areas containing possibly vegetated areas. Sedimentary input from volcanic sources (Mt Morning region) was low with a greater contribution from lithologies exposed in the Transantarctic Mountains, such as the Beacon Supergroup and the Granite Harbor Intrusive.
- (2) Muddy diamictite with low magnetic susceptibility and Nb content (e.g., from 903.06 to 950.55 mbsf; Figure 10g, inset B). Glacial grounding zones advanced into nearshore marine environments. Fast flowing, erosive outlet glaciers carried substantial amounts of sediment into the marine setting. Input of volcanogenic sediment at the AND-2A drill site was low, possibly because material derived from Mt Morning was largely transported north of the AND-2A site by icebergs that began to melt after they had drifted northward along the coast. To support this interpretation, sedimentary clasts that accumulated at the AND-2A drill site under these environmental conditions were primarily derived from the large outlet of glaciers draining areas to the south, the Mulock and Byrd glaciers.
- (3) Sandstone and sandy conglomerate with medium to high magnetic susceptibility and Nb content (e.g., from 950.55 to 965.43 mbsf and in the upper part of LSU 11; Figure 10g, inset C). These intervals represent times when the glacial grounding zones persisted in nearshore marine environments and multi-season sea ice and/or ice shelves fringed the coast. Sediments were derived from proximal volcanic sources and outcrops in the Transantarctic Mountains. Volcanic sediment derived from Mt Morning was transported by wind and accumulated on floating ice that periodically melted, allowing volcanogenic sediment to accumulate at the drill site. This mechanism of deposition in this sandstone-dominated facies was previously hypothesized by Iacoviello et al. (2015) to explain the transport of heavy minerals from the McMVG to the AND-2A drill site. Ohneiser et al. (2015) identified a significant contribution of superparamagnetic grains in modern sediments throughout the region (on land, sea ice, and on the sea floor) and suggested that they are formed in the modern, cold, hyperarid, wind-dominated environment. Our rock magnetic data do not show evidence for a significant contribution of superparamagnetic grains, which may indicate that late early Miocene conditions were less cold than today;
- (4) Sandy diamictite with high magnetic susceptibility and Nb content (e.g., from 1,040 and 1,103.96 mbsf and between about 975 and 995.78 mbsf; Figure 10g, inset D). These units reflect intervals when ice sheets advanced across the inner continental shelf. Locally derived volcanic clasts were deposited proximal to the grounding line of outlet or piedmont glaciers or beneath a floating ice tongue.

8. Conclusions

Environmental magnetic data from the lower AND-2A drill core has helped to constrain the processes by which sediments were delivered to the drill site during the late early Miocene (from ~18.7 to ~20.2 Ma). We observed stratigraphic zones with an alternation of intervals with high magnetic mineral concentration and intervals with very low magnetic mineral concentration with a relatively constant magnetic grain size. This alternation indicates paleoenvironmental differences, with the sourcing of magnetic material, which we interpret to be mostly volcanic in origin, switched on and off as a result of depositional processes controlled primarily by glacial conditions and possibly also by the abundance of volcanic material that could be sourced.

LUs from 778.63 mbsf to the bottom of AND-2A drill core (LSUs 11–14) record marked environmental variability in an ice-distal to ice-proximal depositional environment. We recognize settings varying from subglacial and grounding zone proximal to hemipelagic and neritic under the influence of icebergs and sea ice (Field et al., 2018; Fielding et al., 2011; Levy et al., 2016; Passchier et al., 2011).

Perhaps the most interesting unit is the thick mudstone of LSU 11. Modern studies show that large amounts of volcanic material derived from the McMVG accumulate on the ice shelf and sea ice to the South of the drill site (Chewings et al., 2011). We suggest that similar processes may explain the increase in magnetic mineral concentration observed in this interval, and we link it to a period of cool and relatively stable climate during which a long-standing cover of floating ice developed over the drill site. Strong southerly winds eroded the volcanic edifice to the south and volcanic-clast-rich sediment

accumulated on the floating ice platform above the drill site. Periodic melt of this ice platform delivered the sediment to the sea floor.

Our results support and refine previous environmental interpretations and delineate the complex variability of ice extent during the late early Miocene in the southern McMurdo Sound. This study adds to the growing body of evidence that Antarctica's ice sheet was highly dynamic through most of its history. Further cores, and more work on existing records of a similar age from other regions of the continental margin, are needed to fully characterize such large-scale ice sheet fluctuations and to provide ground truth for the last generation of global climate models.

Acknowledgments

The ANDRILL program is a multinational partnership between Germany, Italy, New Zealand, and the United States. We thank the SMS drillers who recovered the AND-2A core; Robin Frisch-Gleason, Graziano Scotto di Clemente, and Bob Williams who assisted with sample collection; and the SMS curatorial staff for administering the many sample requests and professional core handling. The drilling system was developed by Alex Pyne at Victoria University of Wellington and Webster Drilling and Exploration Ltd in collaboration with Antarctica New Zealand, which is the project operator. Antarctica New Zealand supported the drilling team at Scott Base, and Raytheon Polar Services supported the scientists at McMurdo Station and the Crary Science and Engineering Center. The ANDRILL Science Management Office at the University of Nebraska-Lincoln provided scientific support, and scientific studies were jointly funded by the U.S. National Science Foundation (NSF), NZ Foundation for Research (FRST), the Italian Antarctic Research Program (PNRA), the German Research Foundation (DFG), and the Alfred Wegener Institute for Polar and Marine Research (AWI). L. J. is supported by Fundação de Amparo a Pesquisa do Estado de São Paulo (FAPESP) project 2011/22018-3 and Coordenação de Aperfeiçoamento de Pessoal de Nível Superior (CAPES) project Ciências do Mar II. The data are openly available in PANGAEA at <https://doi.pangaea.de/10.1594/PANGAEA.743270> (whole core images), and <https://doi.pangaea.de/10.1594/PANGAEA.897964> (magnetic properties). Additional data that support the findings of this study are available from the authors upon request.

References

- Acton, G., Crampton, J., Di Vincenzo, G., Fielding, C. G., Florindo, F., Hannah, M. J., et al., & ANDRILL-SMS Science Team (2008). Preliminary integrated chronostratigraphy of the AND-2A core, ANDRILL Southern McMurdo Sound Project, Antarctica. *Terra Antarctica*, 15, 211–220.
- Acton, G., Florindo, F., Jovane, L., Lum, B., Ohneiser, C., Sagnotti, L., et al. (2008). Paleomagnetism of the AND-2A Core, ANDRILL Southern McMurdo Sound Project, Antarctica. In Harwood, D., Florindo, F., Talarico, F., and Levy, R.H. (Eds.), Studies from the ANDRILL Southern McMurdo Sound Project, Antarctica—initial science report on AND-2A. *Terra Antarctica*, 15(1), 193–210.
- Barrett, P. J. (1981). History of the Ross Sea region during the deposition of the Beacon Supergroup 400–180 million years ago. *Journal of the Royal Society of New Zealand*, 11, 447–458.
- Barrett, P. J. (1986). Antarctic Cenozoic history from the MSSTS-1 borehole, McMurdo Sound. *New Zealand Department of Scientific and Industrial Research Bulletin*, 237, 1–174.
- Barrett, P. J. (1989). Antarctic Cenozoic history from the CIROS-1 drillhole, McMurdo Sound. *New Zealand Department of Scientific and Industrial Research Bulletin*, 245, 1–254.
- Barrett, P. J. (1998). Studies from the Cape Roberts Project, Ross Sea, Antarctica: Scientific report of CRP-1, overview. *Terra Antarctica*, 5, 255–258.
- Barrett, P. J., Grindley, G. W., & Webb, P. N. (1972). The Beacon Supergroup of East Antarctica. In R. J. Adie (Ed.), *Antarctic geology and geophysics*, (pp. 319–322). Oslo: Universitetsforlaget.
- Barrett, P. J., Sarti, M., & Wise, S. W. (2000). Studies from the Cape Roberts Project, Ross Sea, Antarctica, scientific results of CRP-2/2A, parts I and II. *Terra Antarctica*, 7(4/5), 1–665.
- Barrett, P. J., Sarti, M., & Wise, S. W. (2001). Studies from the Cape Roberts Project, Ross Sea, Antarctica, scientific results of CRP-3, parts I and II. *Terra Antarctica*, 8(3/4), 1–621.
- Bédard, J. H. J., Marsh, D. B., Hersum, G. T., Naslund, H. R., & Mukasa, B. S. (2007). Large-scale mechanical redistribution of orthopyroxene and plagioclase in the Basement Sill, Ferrar Dolerites, McMurdo Dry Valleys, Antarctica: Petrological, mineral-chemical and field evidence for channelized movement of crystals and melt. *Journal of Petrology*, 48, 2289–2326.
- Bennett, L. H., & Della Torre, E. (2005). Analysis of wasp-waist hysteresis loops. *Journal of Applied Physics*, 97, 10E502. <https://doi.org/10.1063/1.1846171>
- Brachfeld, S., Pinzon, J., Darley, J., Sagnotti, L., Kuhn, G., Florindo, F., et al. (2013). Iron oxide tracers of ice sheet extent and sediment provenance in the ANDRILL AND-1B drill core, Ross Sea, Antarctica. *Global and Planetary Change*, <https://doi.org/10.1016/j.gloplacha.2013.09.015>, 110, 420–433.
- Brancolini, G., Busetti, M., Marchetti, A., De Santis, L., Zanolla, C., Cooper, A. K., et al. (1995). Descriptive text for the seismic stratigraphic atlas of the Ross Sea. In A. K. Cooper, & F. Peter (Eds.), *Barker e Giuliano BrancoliniGeology and seismic stratigraphy of the Antarctic Margin* Antarctic Research Series (Vol. 68, pp. A268–A271). Washington, DC: American Geophysical Union.
- Campbell, I. B., & Claridge, G. G. C. (1987). *Antarctica: Soils, weathering processes and environment, in Developments in soil science* (Vol. 16, p. 368). Amsterdam, Netherlands: Elsevier.
- Cape Roberts Science Team (1999). Studies from the Cape Roberts Project, Ross Sea, Antarctica. initial report on CRP-2/2A. *Terra Antarctica*, 6, 1–173. With Supplement, 245 pp
- Chewings, J. M., Atkins, G. B., Dunbar, G. B., Golledge, N. R., & Alloway, B. V. (2011). Aeolian 'dust' flux in McMurdo Sound, SW Ross Sea, Antarctica. In N. J. Litchfield, & K. Clark (Eds.), Abstract volume, Geosciences Conference, Nelson, 27 November–1 December: *Geoscience Society of New Zealand Miscellaneous Publication v. 130A*.
- Cooper, A. K., Davey, F. J., & Behrendt, J. C. (1987). Seismic stratigraphy and structure of the Victoria Land Basin, western Ross Sea, Antarctica. In A. K. Cooper & F. J. Davey (Eds.), *The Antarctic continental margin: Geology and geophysics of the western Ross Sea: Circum-Pacific Council for Energy and Mineral Resources* (pp. 27–65). Houston, TX: Earth Science Series, 5B.
- Cox, S. C., Turnbull, I. M., Isaac, M. J., Townsend, D. B., & Smith Lytle, B. (2012). Geology of southern Victoria Land Antarctica. Lower Hutt: GNS Science. Institute of Geological & Nuclear Sciences 1:250,000 geological map 22.135 p. + 1 folded map. <https://www.gns.cri.nz/Home/Our-Science/Earth-Science/Regional-Geology/Geological-Maps/1-250-000-Geological-Map-of-Southern-Victoria-Land-Antarctica>.
- Day, R., Fuller, M. D., & Schmidt, V. A. (1977). Hysteresis properties of titanomagnetites: Grain size and composition dependence. *Physics of the Earth and planetary interiors*, 13, 260–266.
- Di Roberto, A., Del Carlo, P., Rocchi, S., Bracciali, L., Di Vincenzo, G., Rocchi, S., & Panter, K. (2012). Early Miocene volcanic activity and paleoenvironment conditions of the AND-2A core (southern McMurdo Sound, Antarctica). *Geosphere*, 8(6), 1342. <https://doi.org/10.1130/GES00754.1>
- Di Vincenzo, G., Bracciali, L., Del Carlo, P., Panter, K., & Rocchi, S. (2010). ^{40}Ar - ^{39}Ar dating of volcanogenic products from the AND-2A core (ANDRILL Southern McMurdo Sound Project, Antarctica): Correlations with the Erebus Volcanic Province and implications for the age model of the core. *Bulletin of Volcanology*, 72, 487–505. <https://doi.org/10.1007/s00445-009-0337-z>
- Dunbar, G., Atkins, C., Magens, D., Niessen, F., & the ANDRILL-SMS Science Team (2008). Physical properties of the AND-2A Core, ANDRILL Southern McMurdo Sound Project, Antarctica. *Terra Antarctica*, 15, 49–56.
- Dunlop, D. J. (2002a). Theory and application of the Day plot (M_{rs}/M_s versus H_{cr}/H_c): 1. Theoretical curves and tests using titanomagnetite data. *Journal of Geophysical Research*, 107(B3), 2056. <https://doi.org/10.1029/2001JB000486>

- Dunlop, D. J. (2002b). Theory and application of the Day plot (M_{rs}/M_s versus H_{cr}/H_c): 2. Application to data for rocks, sediments, and soils. *Journal of Geophysical Research*, 107(B3), 2057. <https://doi.org/10.1029/2001JB000487>
- Elliot, D. H., & Fleming, T. H. (2000). Weddell triple junction: The principal focus of Ferrar and Karoo magmatism during initial breakup of Gondwana. *Geology*, 28, 539–542.
- Elliot, D. H., Fleming, T. H., Kyle, P. R., & Foland, K. A. (1999). Long-distance transport of magmas in the Jurassic Ferrar Large Igneous Province, Antarctica. *Earth and Planetary Science Letters*, 167, 89–104.
- Field, B. D., Browne, G. H., Fielding, C. R., Florindo, F., Harwood, D. M., Judge, S. A., et al. (2018). A sedimentological record of early Miocene ice advance and retreat, AND-2A drill hole, McMurdo Sound, Antarctica. *Geosphere*, 14(4), 1–24. <https://doi.org/10.1130/GES01592.1>
- Fielding, C. R., Atkins, C. B., Basset, K. N., Browne, G. H., Dunbar, G. B., Field, B. D., et al., & the ANDRILL-SMS Science Team (2008). Sedimentology and stratigraphy of the AND-2A core, ANDRILL Southern McMurdo Sound Project, Antarctica. *Terra Antartica*, 15, 77–112.
- Fielding, C. R., Browne, G. H., Field, B. D., Florindo, F., Harwood, D. M., Krissek, L. A., et al. (2011). Sequence stratigraphy of the ANDRILL AND-2A drillcore, Antarctica: A long-term, ice-proximal record of early to mid-Miocene climate, sea-level and glacial dynamism. *Palaeogeography, Palaeoclimatology, Palaeoecology*, 305, 337–351.
- Fielding, C. R., Whittaker, J., Henrys, S. A., Wilson, T. J., & Naish, T. R. (2008). Seismic facies and stratigraphy of the Cenozoic succession in McMurdo Sound, Antarctica: Implications for tectonic, climatic and glacial history. *Palaeogeography, Palaeoclimatology, Palaeoecology*, 260, 8–29.
- Florindo, F., Harwood, D., Levy, R., & SMS Project Science Team (2008). ANDRILL's success during the 4th International Polar Year. *Scientific Drilling*, 6, 29–31. <https://doi.org/10.2204/iodp.sd.6.03.2008>
- Florindo, F., Wilson, G. S., Roberts, A. P., Sagnotti, L., & Verosub, K. L. (2005). Magnetostratigraphic chronology of a late Eocene to early Miocene glacimarine succession from the Victoria Land Basin, Ross Sea, Antarctica. *Global and Planetary Change*, 45, 236–207. <https://doi.org/10.1016/j.gloplacha.2004.09.009>
- Grindley, G. W., & Warren, G. (1964). Stratigraphic nomenclature and correlation in the western Ross Sea region. In R. J. Adie (Ed.), *Antarctic geology* (pp. 314–333). Amsterdam, Netherlands: North Holland Publishing.
- Gunn, B. M., & Warren, G. (1962). Geology of Victoria Land between Mawson and Mullock Glaciers, Antarctica. *New Zealand Geological Survey bulletin*, 71, 1–157.
- Hambrey, M. J., & Barrett, P. J. (1993). Cenozoic sedimentary and climatic record, Ross Sea region, Antarctica. In J. P. Kennett & D. A. Warnke (Eds.), *The Antarctic paleoenvironment: A perspective on global change, part 2*, *Antarctic Research Series* (pp. 91–124). Washington, DC: American Geophysical Union.
- Hambrey, M. J., & Wise, S. W. (1998). Studies from the Cape Roberts Project, Ross Sea, Antarctica, scientific results of CRP-1. *Terra Antartica*, 5(3), 255–713.
- Harrington, H. J. (1958). Nomenclature of rock units in the Ross Sea region, Antarctica. *Nature*, 182, 290.
- Harrison, R. J., & Feinberg, J. M. (2008). FORCinel: An improved algorithm for calculating first-order reversal curve distributions using locally weighted regression smoothing. *Geochemistry Geophysics Geosystems*, 9, Q05016. <https://doi.org/10.1029/2008GC001987>
- Harwood, D., Florindo, F., Talarico, F., Levy, R., Kuhn, G., Naish, T., et al. (2009). Antarctic drilling recovers stratigraphic records from the continental margin. *Eos, Transactions American Geophysical Union*, 90(11). <https://doi.org/10.1029/2009EO110002>
- Henrys, S. A., Wilson, T. J., Whittaker, J. M., Fielding, C. R., Hall, J. M., & Naish, T. (2007). Tectonic history of mid-Miocene to present, southern Victoria Land Basin, inferred from seismic stratigraphy, in McMurdo Sound, Antarctica, in Cooper, A.K., and Raymond C.R. et al., eds., Antarctica: A keystone in a changing world—Online Proceedings of the 10th ISAES, USGS Open-File Report 2007-1047, Short Research Paper 049.
- Heslop, D., & Roberts, A. P. (2012). Estimation of significance levels and confidence intervals for first-order reversal curve distributions. *Geochemistry, Geophysics, Geosystems*, 13, Q12Z40. <https://doi.org/10.1029/2012GC004115>
- Holbourn, A., Kuhnt, W., Kochhann, K. G. D., Andersen, N., & Sebastian, M. K. J. (2015). Global perturbation of the carbon cycle at the onset of the Miocene Climatic Optimum. *Geology*, 43(2), 123–126.
- Holbourn, A. E., Kuhnt, W., Clemens, S. C., Kochhann, K. G. D., Johnck, J., Lubbers, J., & Andersen, N. (2018). Late Miocene climate cooling and intensification of southeast Asian winter monsoon. *Nature Communications*, <https://doi.org/10.1038/s41467-018-03950-1>, 9(1), 1584.
- Holbourn, A. E., Kuhnt, W., Lyle, M. W., Schneider, L. J., Romero, O. E., & Andersen, N. (2014). Middle Miocene climate cooling linked to intensification of eastern equatorial Pacific upwelling. *Geology*, 42(1), 19–22.
- Hunt, C., Moskowitz, B. M., & Banerjee, S. K. (1995). Magnetic properties of rocks and minerals. In T. J. Ahrens (Ed.), *In Rock physics & phase relations: A handbook of physical constants*, AGU Ref. Shelf (Vol. 3, pp. 189–204). Washington, DC: American Geophysical Union. <https://doi.org/10.1029/RF003p0189>
- Iacoviello, F., Giorgetti, G., Nieto, F., & Turbanti Memmi, I. (2012). Evolution with depth from detrital to authigenic smectites in sediments from AND-2A drill core (McMurdo Sound, Antarctica). *Clay Minerals*, 47, 481–498. <https://doi.org/10.1180/claymin.2012.047.4.07>
- Iacoviello, F., Giorgetti, G., Turbanti Memmi, I., & Passchier, S. (2015). Early Miocene Antarctic glacial history: New insights from heavy mineral analysis from ANDRILL AND-2A drill core sediments. *International Journal of Earth Sciences*, 104(3), 853–872. <https://doi.org/10.1007/s00531-014-1117-3>
- John, C. M., Karner, G. D., Browning, E., Leckie, R. M., Mateo, Z., Carson, B., & Lowery, C. (2011). Timing and magnitude of Miocene eustasy derived from the mixed siliciclastic-carbonate stratigraphic record of the northeastern Australian margin. *Earth and Planetary Science Letters*, 304(3–4), 455–467.
- Kharwanlang, R. S., & Shukla, P. (2012). Analysis of wasp-waisted hysteresis loops in magnetic rocks. *Physical Review E*, 85, 011124. <https://doi.org/10.1103/PhysRevE.85.011124>
- Kominz, M. A., Browning, J. V., Miller, K. G., Sugarman, P. J., Mizintseva, S., & Scotesce, C. R. (2008). Late Cretaceous to Miocene sea-level estimates from the New Jersey and Delaware coastal plain coreholes: An error analysis. *Basin Research*, 20, 211–226. <https://doi.org/10.1111/j.1365-2117.2008.00354.x>
- Kominz, M. A., Miller, K. G., Browning, J. V., Katz, M. E., & Mountain, G. S. (2016). Miocene relative sea level on the New Jersey shallow continental shelf and coastal plain derived from one-dimensional backstripping: A case for both eustasy and epirogeny. *Geosphere*, 12, 1437–1456. <https://doi.org/10.1130/ges01241.1>
- Kyle, P. R. (1990). McMurdo volcanic group-western Ross embayment: Introduction. *Antarctic Research Series*, 48, 19–25.
- Lear, C. H., Rosenthal, Y., Coxall, H. K., & Wilson, P. A. (2004). Late Eocene to early Miocene ice sheet dynamics and the global carbon cycle. *Paleoceanography*, 19, PA4015. <https://doi.org/10.1029/2004pa001039>

- Levy, R. H., Harwood, D., Florindo, F., Sangiorgi, F., Tripati, R., von Eynatten, H., et al. (2016). Antarctic ice sheet sensitivity to atmospheric CO₂ variations in the early to mid-Miocene. *Proceedings of the National Academy of Sciences of the United States of America*, *113*, 3453–3458. <https://doi.org/10.1073/pnas.1516030113>
- Lewis, A. R., & Ashworth, A. C. (2015). An early to middle Miocene record of ice-sheet and landscape evolution from the Friis Hills Antarctica. *Geological Society of America Bulletin*, *128*, 719–738. <https://doi.org/10.1130/B31319.1>
- Lewis, A. R., Marchant, D. R., Ashworth, A. C., Hemming, S. R., & Machlus, M. L. (2007). Major middle Miocene global climate change: Evidence from East Antarctica and the Transantarctic Mountains. *Geological Society of America Bulletin*, *119*(11/12), 1449–1461. <https://doi.org/10.1130/B26134.1>
- Liebrand, D., de Bakker, A. T. M., Beddow, H. M., Wilson, P. A., Bohaty, S. M., Ruessink, G., et al. (2017). Evolution of the early Antarctic ice ages. *Proceedings of the National Academy of Sciences*, *114*, 3867–3872. <https://doi.org/10.1073/pnas.1615440114>
- Liu, Q., Roberts, A. P., Larrasoña, J. C., Banerjee, S. K., Guyodo, Y., Tauxe, L., & Oldfield, F. (2012). Environmental magnetism: Principles and applications. *Reviews of Geophysics*, *50*, B10103. <https://doi.org/10.1029/2012RG000393>
- Marchant, D. R., Denton, G. H., Swisher, C. C. III, & Potter, N. P. Jr. (1996). Late Cenozoic Antarctic paleoclimate reconstructed from volcanic ashes in the Dry Valleys region of Southern Victoria Land. *Geological Society of America Bulletin*, *108*, 181–194. [https://doi.org/10.1130/0016-7606\(1996\)108<0181:LCAPRF>2.3.CO;2](https://doi.org/10.1130/0016-7606(1996)108<0181:LCAPRF>2.3.CO;2)
- Miller, K. G., Mountain, G. S., & Leg 150 Shipboard Party, & Members of the New Jersey Coastal Plain Drilling Project (1996). Drilling and dating New Jersey Oligocene–Miocene sequences. Ice volume, global sea level, and exxon records. *Science*, *271*, 1092–1095.
- Miller, K. G., Wright, J. D., & Fairbanks, R. G. (1991). Unlocking the ice house: Oligocene–Miocene oxygen isotopes, eustasy and margin erosion. *Journal of Geophysical Research*, *96*, 6829–6848.
- Naish, T., Powell, R., Levy, R., Florindo, F., Harwood, D., Kuhn, G., et al. (2007). A record of Antarctic climate and ice sheet history recovered. *Eos, Transactions American Geophysical Union*, *88*, 557–558. <https://doi.org/10.1029/2007eo500001>
- Nyland, R. E., Panter, K. S., Rocchi, S., Di Vincenzo, G., Del Carlo, P., Tiepolo, M., et al. (2013). Volcanic activity and its link to glaciation cycles: Single-grain age and geochemistry of early Miocene volcanic glass from ANDRILL AND-2A core, Antarctica. *Journal of Volcanology and Geothermal Research*, *250*, 106–128.
- Ohneiser, C., Wilson, G. W., & Cox, S. C. (2015). Characterisation of magnetic minerals from southern Victoria Land Antarctica. *New Zealand Journal of Geology and Geophysics*, *58*, 52–65. <https://doi.org/10.1080/00288306.2014.990044>
- Passchier, S., Browne, G., Field, B., Fielding, C. R., Krissek, L. A., Panter, K., Pekar, S. F., & ANDRILL-SMS Science Team (2011). Early and middle Miocene Antarctic glacial history from the sedimentary facies distribution in the AND-2A drill hole, Ross Sea, Antarctica. *Geological Society of America Bulletin*, *123*, 2352–2365.
- Passchier, S., Falk, C. J., & Florindo, F. (2013). Orbitally paced shifts in the particle size of Antarctic continental shelf sediments in response to ice dynamics during the Miocene climatic optimum. *Geosphere*, *9*, 54–62. <https://doi.org/10.1130/GES00840.1>
- Pekar, S., & DeConto, R. M. (2006). High-resolution ice-volume estimates for the early Miocene: Evidence for a dynamic ice sheet in Antarctica. *Palaeogeography, Palaeoclimatology, Palaeoecology*, *231*, 101–109. <https://doi.org/10.1016/j.palaeo.2005.07.027>
- Roberts, A. P., Wilson, G. S., Harwood, D. M., & Veresub, K. L. (2003). Glaciation across the Oligocene–Miocene boundary in southern McMurdo Sound, Antarctica: New chronology from the CIROS-1 drill hole. *Palaeogeography, Palaeoclimatology, Palaeoecology*, *198*, 113–130.
- Roberts, A. P., Heslop, D., Zhao, X., & Pike, C. R. (2014). Understanding fine magnetic particle systems through use of first-order reversal curve diagrams. *Reviews of Geophysics*, *52*, 557–602. <https://doi.org/10.1002/2014RG000462>
- Roberts, A. P., Pike, C. R., & Veresub, K. L. (2000). First- order reversal curve diagrams: A new tool for characterizing the magnetic properties of natural samples. *Journal of Geophysical Research*, *105*, 28,461–28,475. <https://doi.org/10.1029/2000JB900326>
- Roberts, A. P., Sagnotti, L., Florindo, F., Bohaty, S. M., Veresub, K. L., Wilson, G. S., & Zachos, J. C. (2013). Environmental magnetic record of paleoclimate, unroofing of the Transantarctic Mountains, and volcanism in late Eocene to early Miocene glaci-marine sediments from the Victoria Land Basin Ross Sea, Antarctica. *Journal of Geophysical Research: Solid Earth*, *118*, 1845–1861. <https://doi.org/10.1002/jgrb.50151>
- Roberts, A. P., Wilson, G. S., Florindo, F., Sagnotti, L., Veresub, K. L., & Harwood, D. M. (1998). Magnetostratigraphy of lower Miocene strata from the CRP-1 core, McMurdo Sound, Ross Sea, Antarctica. *Terra Antartica*, *5*, 703–713.
- Roser, B. P., & Pyne, A. R. (1989). In P. J. Barrett (Ed.), *Wholerock geochemistry. Antarctic Cenozoic history from the CIROS-1 Drillhole, McMurdo Sound, DSIR Bulletin* (pp. 175–184). Wellington, New Zealand), 245: DSIR Publishing.
- Sagnotti, L., Florindo, F., Veresub, K. L., Wilson, G. S., & Roberts, A. P. (1998). Environmental magnetic record of Antarctic palaeoclimate from Eocene–Oligocene glaciomarine sediments, Victoria Land margin. *Geophysical Journal International*, *134*, 653–662.
- Sagnotti, L., Florindo, F., Wilson, G. S., Roberts, A. P., & Veresub, K. L. (1998). Environmental magnetism of lower Miocene strata from the CRP-1 core, McMurdo Sound, Antarctica. *Terra Antartica*, *5*, 661–667.
- Sagnotti, L., Roberts, A. P., Weaver, R., Veresub, K. L., Florindo, F., Wilson, G. S., et al. (2005). Apparent magnetic polarity reversals due to remagnetization resulting from late diagenetic growth of greigite from siderite. *Geophysical Journal International*, *160*, 89–100.
- Sandroni, S., & Talarico, F. M. (2004). Petrography and provenance of basement clasts in CIROS-1 core, McMurdo Sound, Antarctica. *Terra Antartica*, *11*, 93–114.
- Shevenell, A. E., Kennett, J. P., & Lea, D. W. (2008). Middle Miocene ice sheet dynamics, deep-sea temperatures, and carbon cycling: A Southern Ocean perspective. *Geochemistry, Geophysics, Geosystems*, *9*, Q02006. <https://doi.org/10.1029/2007gc001736>
- Smellie, J. L. (2000). Subglacial eruptions. In H. Sigurdsson (Ed.), *Encyclopedia of Volcanoes*, (pp. 403–418). San Diego, CA: Academic Press.
- Veresub, K. L., Florindo, F., Sagnotti, L., Roberts, A. P., & Wilson, G. S. (2000). Environmental magnetism of Oligocene–Miocene glaciomarine strata from the CRP-2/2A drillcore, Victoria Land Basin, Antarctica. *Terra Antartica*, *7*, 599–608.
- Wilch, T. I., Lux, D. R., Denton, G. H., & McIntosh, W. C. (1993). Minimal Pliocene–Pleistocene uplift of the Dry Valleys sector of the Transantarctic Mountains: A key parameter in ice sheet reconstructions. *Geology*, *21*, 841–844.
- Wilson, G., Levy, R., Naish, T., Powell, R., Florindo, F., Ohneiser, C., et al. (2012). Neogene tectonic and climatic evolution of the western Ross Sea, Antarctica—Chronology of events from the AND-1B drillhole. *Global and Planetary Change*, *96*–*97*, 189–203.
- Wilson, G. S., Bohaty, S. M., Fielding, C. R., Florindo, F., Hannah, M. J., Harwood, D. M., et al. (2000). Chronostratigraphy of CRP-2/2A, Victoria Land Basin, Antarctica. *Terra Antartica*, *7*, 647–654.
- Wilson, G. S., Florindo, F., Sagnotti, L., Veresub, K. L., & Roberts, A. P. (2000). Magnetostratigraphy of Oligocene–Miocene glaciomarine strata from the CRP-2/2A core, McMurdo Sound, Ross Sea, Antarctica. *Terra Antartica*, *7*, 631–646.
- Wilson, G. S., Lavelle, M., McIntosh, W. C., Roberts, A. P., Harwood, D. M., Watkins, D. K., et al. (2002). Integrated chronostratigraphic calibration of the Oligocene–Miocene boundary at 24.0+/-0.1 Ma from the CRP-2A drill core, Ross Sea, Antarctica. *Geology*, *30*(11), 1043–1046. [https://doi.org/10.1130/0091-7613\(2002\)030<1043:ICCOTO>2.0.CO;2](https://doi.org/10.1130/0091-7613(2002)030<1043:ICCOTO>2.0.CO;2)

- Zachos, J., Pagani, M., Sloan, L., Thomas, E., & Billups, K. (2001). Trends, rhythms, and aberrations in global climate 65 Ma to present. *Science*, 292(5517), 686–693. <https://doi.org/10.1126/science.1059412>
- Zattin, M., Andreucci, B., Thomson, S. N., Reiners, P. T., & Talarico, F. M. (2012). New constraints on the provenance of the ANDRILL AND-2A succession (western Ross Sea, Antarctica) from apatite triple dating. *Geochimica, Geophysica, Geosystems*, 13, Q10016. <https://doi.org/10.1029/2012GC004357>
- Zavala, K., Leitch, A. M., & Fisher, G. W. (2011). Silicic segregations of the Ferrar Dolerite sills, Antarctica. *Journal of Petrology*, 52(10), 1927–1964. <https://doi.org/10.1093/petrology/egr035>